J Mater Sci: Mater Med (2008) 19:1861–1869
DOI 10.1007/s10856-007-3248-6

On the biocompatibility of a novel Ti-based amorphous composite: structural characterization and in-vitro osteoblasts response

H. Lefaix · A. Asselin · P. Vermaut · J.-M. Sautier · A. Berdal · R. Portier · F. Prima

Received: 9 January 2007 / Accepted: 26 July 2007 / Published online: 4 October 2007

Abstract Titanium and its alloys are frequently used as dental and orthopaedic implants due to their high mechanical strength, low elastic modulus and biocompatibility. However, as these materials have a poor wear resistance, tribo-chemical reactions during use produce debris accumulation, resulting in adverse cellular responses. In that sense, amorphous based materials are potential candidates, considering their hardness and crack growth resistance. This paper reports on the structural characterization of the as-quenched $Ti_{45}Zr_{38}Ni_{17}$ alloy. This system displays a duplex structure never mentioned before with a low dispersion of nanometric beta-phase particles in an amorphous matrix. Moreover, in order to explore the biocompatibility of such composite, primary osteoblasts cultures are used to analyse cell behaviour around and upon the metallic surface. Osteoblasts attach and proliferate on the material as demonstrated by scanning electron microscopy. Cell proliferation and bone nodule formation are also observed in cultures with $Ti_{45}Zr_{38}Ni_{17}$ particles by phase contrast microscope. In addition, transmission electron microscopy reveals ultrastructural features very close to those observed in vivo during intramembranous ossification with active osteoblasts surrounded by an extracellular matrix and a mineralized one. In conclusion, these results demonstrate that osteoblasts, cultured in presence of $Ti_{45}Zr_{38}Ni_{17}$ alloy, proliferate, differentiate and synthesize bone matrix.

H. Lefaix (✉) · P. Vermaut · R. Portier · F. Prima
Laboratoire de Physico-Chimie des Surfaces, CNRS-ENSCP (UMR 7045), Ecole Nationale Supérieure de Chimie de Paris, 11 rue Pierre et Marie Curie, Paris cedex 05 75231, France
e-mail: helene-lefaix@enscp.fr

A. Asselin · J.-M. Sautier · A. Berdal
Centre de Recherche des Cordeliers, Université Pierre et Marie Curie-Paris 6, UMR S872, Paris 75006, France

A. Asselin · J.-M. Sautier · A. Berdal
Université Paris Descartes, UMR S872, Paris 75006, France

A. Asselin · J.-M. Sautier · A. Berdal
INSERM, U872, Paris 75006, France

1 Introduction

The biocompatibility of orthopaedic or dental implants largely depends on the effect of the device on bone-forming cells, namely osteoblasts. A stable connection between material surface and the surrounding tissue is one of the prerequisites for the long-term success of such implants [1, 2]. Moreover, biomaterials must also have mechanical properties and chemical stability well adapted to such constraining biological environment in term of dynamic strains and corrosion. Titanium (Ti) and its alloys are thus widely used in dental and orthopaedic fields because of their exceptional combination of structural and chemical properties [3–6]. Nevertheless, as these materials have a poor wear resistance [2], tribo-chemical reactions during use produce wear debris accumulation which results in adverse cellular response leading to inflammation, release of cytokines, bone cell lysis and thereafter implant loosening [7, 8]. Up to now, in order to improve the wear resistance of these crystalline Ti-based implants, the research has mostly focused on surface treatments such as carbide [9] or TiO_2 [2, 10] coatings and nitridation [2, 11–13], but modifying microstructures of these devices could also be used to modulate their mechanical characteristics. Hence, these last forty years of intense studies about metallic glasses have highlighted an unexpected

combination of properties (i.e. corrosion resistance, high tensile strength, low elastic modulus) [14]. Furthermore, it is known that the precipitation of nanometric particles (crystals or quasicrystals) in the glassy matrix can largely improve its mechanical properties, increasing fracture toughness, hardness and ductility [15–17]. Attractive applications would be reachable in case of good biocompatibility of these peculiar systems, since cells are now known to be sensitive to crystallographic materials organisation [18] and to subtle differences in surface composition [19].

From recent works [20–22], Ti/Zr-based alloys prepared by rapid solidification methods seem to have a tendency to form amorphous phases. This paper reports on preliminary investigations of $Ti_{45}Zr_{38}Ni_{17}$ biocompatibility with respect to its unusual microstructure. This alloy presents fundamental interest due to its ability to promote non periodical microstructures [23–27], as well as presence of biocompatible Zr and Ti alloying elements [2], providing a protective mixed TiO_2/ZrO_2 oxide layer [28]. After structural identification of rapidly quenched (planar flow casting) $Ti_{45}Zr_{38}Ni_{17}$ ribbons, using transmission electron microscopy (TEM) and X-ray diffraction (XRD), cells behaviour has been investigated. Since osteogenic cells are known to be able to proliferate in vitro and to differentiate into mature osteoblasts [29, 30], freshly isolated primary bone-cells are used to evaluate the biocompatibility of Ti–Zr–Ni system. Short- and long-term studies, either in presence of metallic particles or directly in contact with its surface, have been performed using phase contrast microscopy and electron microscopies.

2 Materials and methods

2.1 Material elaboration and structure examination

Ingots of $Ti_{45}Zr_{38}Ni_{17}$ were prepared by arc melting the commercially pure Ti (99.9%), Zr (99.9%) and Ni (99.9%) metals in an argon gas atmosphere. The master alloys were re-melted several times in order to achieve chemical homogeneity. Rapidly solidified ribbons of 10 mm in width and 30–50 μm in thickness were obtained under vacuum by planar flow casting on a rotating copper wheel using a quartz nozzle with controlled ejection temperature of 1300 °C and wheel speed of 36 m s^{-1}. It was estimated from these parameters that the quenching rate was about 10^6 K s^{-1}.

The as-quenched ribbon was structurally characterised by X-ray diffraction (XRD) in a θ-2θ diffractometer (Philips 1810) using Cu–K_α radiation (λ = 0.15418 nm) and by transmission electron microscopy (TEM). Conventional TEM was carried out in a JEOL-2000 EX microscope operating at 200 kV. High resolution transmission electron micrographs (HRTEM) were taken on a JEOL-2010 F instrument (200 kV). TEM specimens were thinned by ion milling techniques under argon gas atmosphere.

2.2 Material elaboration

Two kinds of cell cultures were hereby performed: one with $Ti_{45}Zr_{38}Ni_{17}$ powder, the other with 1 cm^2 plates. Prior to any experiments with cells, all materials are prepared. The 100–800 μm powder was obtained by milling pieces of $Ti_{45}Zr_{38}Ni_{17}$ ribbon with an agate mortar. The 1 cm^2 samples were degreased with a solution of acetone/water (50/50), then ultrasonically cleaned in ethanol and finally dried in dry nitrogen flow. Powder and squares were sterilized by dry heat at 180 °C for 2 h in a furnace.

2.3 Cells and cell culture conditions

Osteoblastic cells were enzymatically isolated from calvaria of neonatal (21 days) Sprague Dawley rats. Briefly, calvaria were aseptically dissected and fragments were digested in phosphate buffered solution with collagenase.

The cells were grown in D Modified Eagle Medium (DMEM, Invitrogen ®), supplemented with ascorbic acid (50 μg/mL, Sigma ®), 10 mM β-glycerophosphate (Sigma ®), 50 UI/mL Penicillin-Streptomycin (Gibco ®) and 10% fetal calf serum (Invitrogen ®). The cells were maintained at 37 °C in a fully humidified atmosphere at 5% CO_2 in air. The media was changed every 48 h. After 3 days in culture, the cells were passaged with Trypsin-EDTA (Gibco-BRL ®), counted by Malassez and plated at a density of 10^5 cells/mL in 60 mm Ø Petri dishes. The $Ti_{45}Zr_{38}Ni_{17}$ particles of size ranging from 100 to 800 μm was added (20 mg/culture dishes) to the wells after 24 h at subconfluence. Other experiments were performed using osteoblasts cultured directly on 1 cm^2 $Ti_{45}Zr_{38}Ni_{17}$ squares.

2.4 Transmission electron microscopy (TEM)

The cells cultured with $Ti_{45}Zr_{38}Ni_{17}$ powder were fixed on day 11 in Karnovsky solution (4% paraformaldehyde, 1% glutaraldehyde) for 1 h and rinsed in 0.2 M sodium cacodylate buffer (pH 7.4). Cell cultures were post-fixed for 1 h in osmium tetroxide diluted in 0.2 M sodium cacodylate buffer, then deshydrated in graded series of ethanol and left overnight in a mixture of absolute ethanol and epon 1:1. The next day the cells were embedded in Epon Araldite and incubated at 60 °C for 1 day. Semi-thin sections were cut,

perpendicularly to the cells layers with a diamond knife. Since it was impossible to perform sections through the metallic particles, we observed the overall structural organisation of the cells and the extracellular matrix neighbouring particles. Thereafter, sections were mounted on glass slides, stained with methylene blue (Azur III), and then examined under light microscopy for orientation purposes. Ultra thin sections were performed, collected on copper grids, and stained with 5% uranyl acetate in water for 4 min and lead citrate for 2 min. The sections were then examined under a TEM (Philips CM-12).

2.5 Scanning electron microscopy (SEM)

The cells cultured on $Ti_{45}Zr_{38}Ni_{17}$ samples were fixed after 4, 24 and 48 h in Karnovsky solution (4% paraformaldehyde, 1% glutaraldehyde) for 1 h and rinsed in 0.2 M sodium cacodylate buffer (pH 7.4). Samples were then deshydrated with ethanol and critical point dried in CO_2. Dried samples were coated with 3 nm Au/Pd and examined using JEOL JSM 6100 scanning electron microscope (SEM) operating with a 15 kV accelerating voltage.

3 Results

3.1 Structural characterization of the as-quenched ribbon

The XRD pattern of the as-quenched $Ti_{45}Zr_{38}Ni_{17}$ (Fig. 1) presents the superposition of characteristic beta phase (β) peaks over an amorphous halo. The two diffraction peaks are assigned to $(110)_\beta$ and $(220)_\beta$.

The representative electron diffraction pattern of this ribbon (Fig. 2a) shows a continuous diffuse circle with bright tiny spots corresponding to a dispersion of randomly orientated nanocrystalline particles. On the bright-field image (Fig. 2b), it can be noticed that the matrix consists mostly of slight dispersion of particles with different crystallographic orientations. Their mean size is around 100 nm in diameter. In addition they display a remarkable speckled morphology (Fig. 2c, d), suggesting that the internal organisation is not homogeneous but composed by juxtaposed and slightly misoriented crystalline zones.

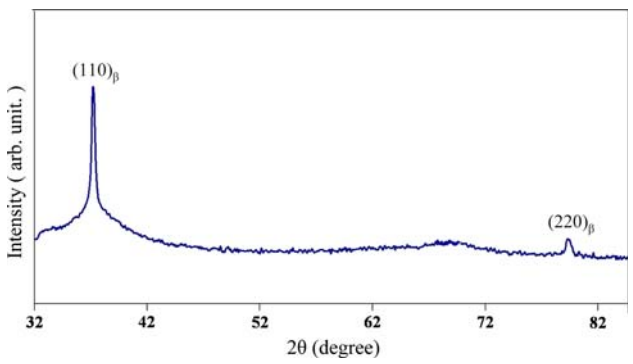

Fig. 1 XRD pattern of the as-quenched $Ti_{45}Zr_{38}Ni_{17}$ ribbon (Cu Kα $\lambda = 0.15418$ nm) showing the superposition of characteristic beta phase peaks over an amorphous halo

Figure 3a is the HRTEM image obtained at the interface between the matrix and a particle. It can be observed that the crystalline structure in the precipitate is lost in the matrix. This confirms the amorphous nature of this latter although particles are crystalline. In the Fourier transform spectrum (Fig. 3b), it is possible to distinguish spots associated with a [100] zone axis orientation, feature of a bcc phase. This assumption is strongly supported by diffractions from the particles which show 6-fold (Fig. 3c) and 4-fold (Fig. 3d) axes, consistent with bcc β-phase structure.

3.2 Cell cultures

3.2.1 Phase contrast microscopy

The primary cells are seeded at a density of 10^5 cells/mL at passage 1. Phase contrast microscopy shows that 4 h later, the cells start to attach and spread on the culture dishes (data not shown). The next day, the metallic particles of size ranging from 100 to 800 µm are added to the culture medium: cells adhering on the culture dishes exhibit a polygonal morphology, known as phenotypic feature of osteoblasts (Fig. 4a).

After a proliferative phase, the cells reach confluence by days 2–3 of culture (Fig. 4b), immobilizing particles in the cell layer and forming multicellular layers, evidenced by the refringent collar around the powder.

From day 7 of culture, morphological changes are noted in some areas and refractile clusters of cells become easily identifiable (Fig. 4c). These bright condensations, composed of tight cellular aggregates, increase in number during the next days. Condensations mark the onset of osteoblasts differentiation programme and are followed on day 11 by the formation of sporadically dispersed darker nodules (Fig. 4d).

3.2.2 Transmission electron microscopy

Transmission electron microscopy allows visualization of the ultrastructural organisation of cells and the extracellular matrix around the metallic particles. At day 11 of culture, TEM observations reveal a osteoblasts surrounded by an extracellular matrix, composed of densely packed collagen

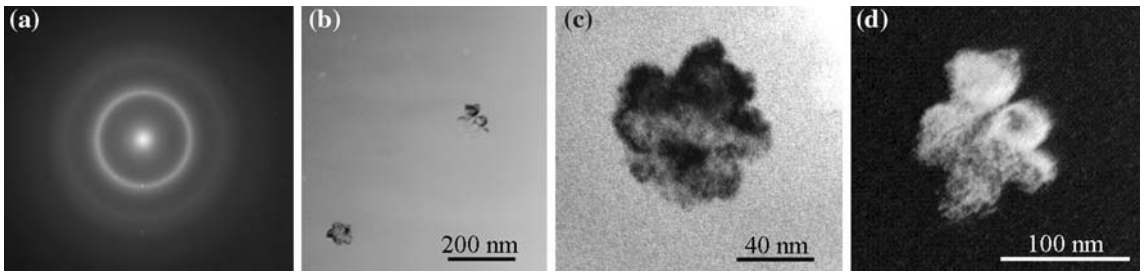

Fig. 2 TEM analysis of the as-quenched $Ti_{45}Zr_{38}Ni_{17}$ alloy: (**a**) Selected Area Diffraction Pattern, (**b**) and (**c**) bright field images of nanometric β phase particles, (**d**) dark field image of a nanometric β phase particles in amorphous matrix

either cut in transversal or longitudinal sections (Fig. 5a). The unmineralized osteoid matrix and the mineralized bone matrix are separated by a mineralized front. At higher magnification, it is possible to observe needle-shape crystals close to the mineralization front, corresponding to bone nucleation sites (Fig. 5b). In addition, mineralized foci could be dispersed among the collageneous matrix.

3.2.3 Scanning electron microscopy

In order to examine the direct influence of $Ti_{45}Zr_{38}Ni_{17}$ surface on osteoblastic behaviour, cells are directly plated on metallic squares and Thermanox® coverslips, used as controls.

SEM observations show that, after 4 h of culture, osteoblasts adhere to their substrates by mean of thin cytoplasmic digitations (filopodia) or larger ones, namely lamellipodia (Fig. 6a). Cells are flattened so that the substrate's morphology is visible through some of them. They look as if they were integrated in the relief, developing thus very intimate contact with $Ti_{45}Zr_{38}Ni_{17}$. Furthermore, it is possible to observe the presence of small spherical structures ranging in size from 100 to 500 nm on the dorsal surface of cells.

After 24 h, almost the entire surface is covered by a subconfluent cellular layer since osteoblasts have proliferated, largely increasing the density of cells (Fig. 6b). Most of flattened cells do not show any specific orientation: they look scattered in all directions with similar structures in term of filopodia and lamellipodia. Nevertheless, some osteoblasts display a polarized structure with clear distinction between cell front and rear, feature of cell motivivity. We can also observe that in the close of the grooves present on this surface, cells tend to bridge over them. Cell-substratum contact is thus confined to the ridge surfaces between the grooves. Finally, osteoblasts have developed an important network of intercellular communication.

After 48 h, the cellular layer is confluent so that most of individual cells can not be identified. The proliferative stage is not finished but, as cells are more numerous, their morphology is changing from polygonal to more elongated. It is possible to observe dense cellular interconnections between osteoblasts, among which lots have buds on their cytoskeleton (Fig. 6c).

4 Discussion

Recent works have shown that cells are sensitive to crystallographic materials organisation [18]. However, although hypotheses could be made about the sensitivity of cells to the absence of long-range organisation, feature of amorphous phase, their behaviour with respect to such non periodic structure has not been studied so far.

Rapid solidification techniques as planar flow casting prevent the hot metallic liquid from primary crystallisation when quenched. In some systems (Al-based or Zr-based mainly), quasicrystalline (QC) structures can be reached, conferring special properties to these so-obtained materials [33–35]. In that context, a set of alloys based on the Ti–Zr–Ni ternary system has been designed by Kelton et al. [36, 37] for their potential catalytic activity (hygrogen storage [38, 39]) due to a stable icosahedral QC phase precipitation. Moreover, it has been showed that different preparation techniques such as ball milling, suction casting or gas atomization promote complex microstructures like QC, approximants and Lave phases. Increasing the cooling rate up to 10^6 K s^{-1}, using planar flow casting, results in the formation of amorphous structures. In this study, $Ti_{45}Zr_{38}Ni_{17}$ system has been structurally investigated in its as-quenched state. From XRD and TEM observations, the so-obtained microstructure mainly corresponds to the dispersion of β particles in an amorphous phase. The lattice constant of this body-centered cubic (bcc) phase, a_β = 0.341 nm, evaluated from the $(110)_\beta$ and $(220)_\beta$ diffraction peaks shift, matches parameters mentioned elsewhere for a Ti/Zr solid solution [24]. Moreover, the absence of

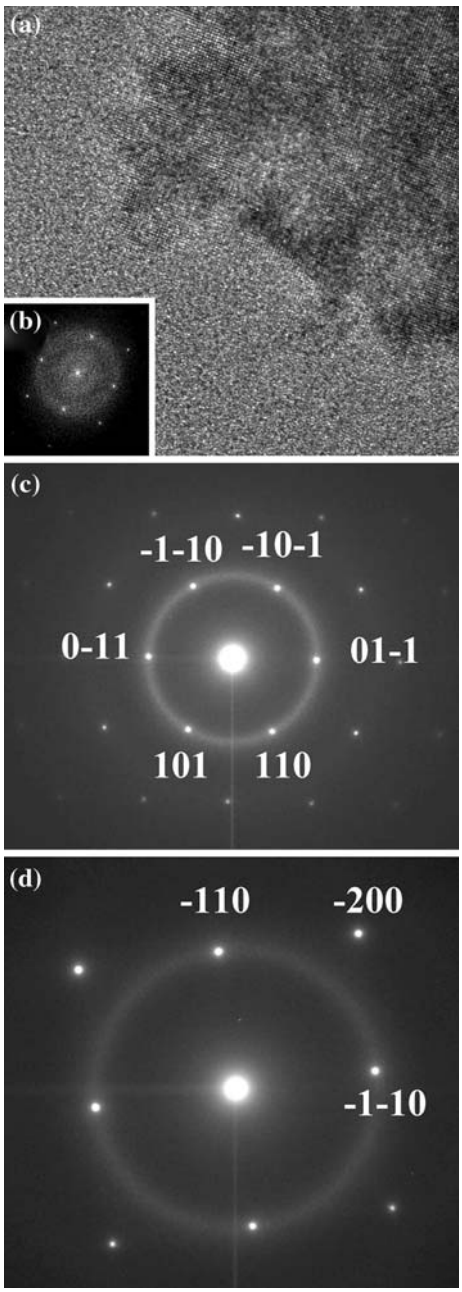

Fig. 3 TEM analysis of the as-quenched $Ti_{45}Zr_{38}Ni_{17}$ alloy: (**a**) HRTEM image of the interface between the amorphous matrix and a β crystalline particle observed along the $[100]_\beta$ axis, (**b**) Fourier transform spectrum of the image (**a**), (**c**, **d**) nanobeam diffraction patterns of a crystalline particle along the $[-111]_\beta$ zone axis (six-fold symmetry) and the $[100]_\beta$ zone axis (four-fold symmetry) respectively

$(200)_\beta$ and $(211)_\beta$ diffraction peaks is probably due to the solidification technique: planar flow casting may create a strong thermal gradient, leading to the final crystallographic texture. No additional phase seems to coexist, neither C14-type Laves phase, nor intermetallic precipitates, as reported elsewhere [24]. Such a duplex structure has not been previously mentioned in this ternary system since planar flow casted alloys quenching rates are two orders of magnitude higher compared to powder metallurgy techniques such as gas atomization [40].

Before exploring structural effects of amorphous nanocrystallized $Ti_{45}Zr_{38}Ni_{17}$ on cell behaviour, the first step is to validate this novel composition, never immersed in a biological environment. Recent works from our laboratory [28] showed that the native oxide layer, covering this material, is mainly composed of ZrO_2 and TiO_2. Hence, experiments around and upon metallic surfaces have been performed to highlight possible chemical effects of the ternary Ti–Zr–Ni alloy on osteogenic cells. The reason we used these primary cultures is their capacity to proliferate and differentiate along the osteoblastic pathway in the presence of ascorbic acid and β-glycerophosphate. Since cellular morphology is an accepted parameter in biocompatibility tests [3, 41], cells are hereby analysed in term of morphological appearance and growth properties.

From phase contrast micrographs, it has been observed that osteoblastic cells can adhere on the culture dish, grow and proliferate in presence of $Ti_{45}Zr_{38}Ni_{17}$ particles. Their morphology and organisation as condensed cellular clusters (day 7 of culture) demonstrate the absence of cytotoxical effects from the metallic material. At day 11, the darker nodules in the cell layer are assigned to the occurrence of mineralization [42, 43], evidence of normal osteoblasts development as well [44]. Thus, up to 19 days, chronological events (adhesion, proliferation, differentiation) in bone metabolism are not modified by the dispersion of metallic particles in the medium. The same phase contrast microscopy observations were obtained with bioactive glasses in contact with the pre-osteoblastic cell line MC3T3 [45], known to be able to differentiate in vitro as well. Authors concluded about the biocompatibility of the material and its ability to support the growth of osteoblasts-like cells in vitro. On the same way, we can conclude about the lack of cytotoxicity of $Ti_{45}Zr_{38}Ni_{17}$ since no cellular debris in the culture medium is detected at any time of the experiment. Furthermore, TEM observations reveal a histological organization very close to what observed in vivo during intramembranous ossification and similar to those obtained in presence of bioactive glass [45] or Ti-based biomaterials [46]. The formation of mineralized matrix is of great importance as an evidence of favourable environment for bone deposition. $Ti_{45}Zr_{38}Ni_{17}$ particles are not only biocompatible but also cytocompatible with respect to osteoblastic differentiation.

Although $Ti_{45}Zr_{38}Ni_{17}$ doesn't affect cells development at distance, biocompatibility of materials is really defined when contacts exist between the surface and biological materials. Thus, it is widely reported that the performance of biomaterial depends on how cells and proteins interact

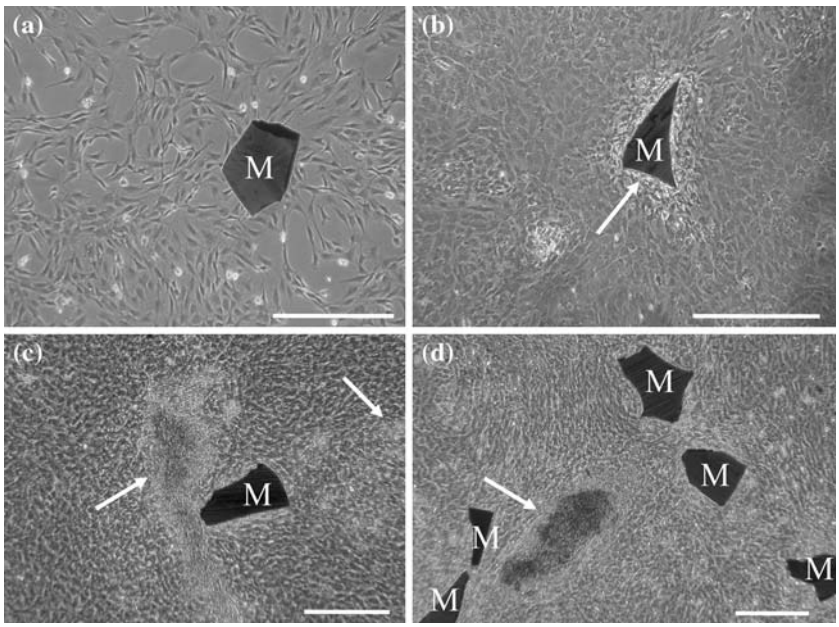

Fig. 4 Observation by phase contrast microscopy of osteoblastic cells, cultured with $Ti_{45}Zr_{38}Ni_{17}$ powder. (**a**) at day 0 (just after addition of metallic particles), cells display a polygonal morphology. (Bar = 400 μm), (**b**) at day 3, cells have reached the confluence. A refringent collar is visible around the particle (arrow head). (Bar = 400 μm), (**c**) at day 7, zones of cellular differentiation are seen as discrete bright patch around and at distance of the powder (arrow head). (Bar = 200 μm), (**d**) at day 11, mineralized nodules are seen in the culture medium as darker zone (arrow head). (Bar = 200 μm). M = $Ti_{45}Zr_{38}Ni_{17}$ powder

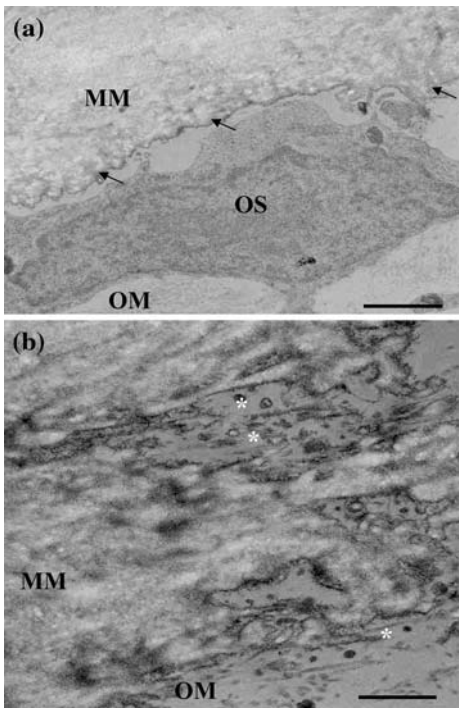

Fig. 5 TEM observations of osteoblastic cells, cultured with $Ti_{45}Zr_{38}Ni_{17}$ particles, at day 11. (**a**) An osteoblast (OS) is surrounding by an extracellular matrix, composed of densely packed collagen fibers. A mineralized matrix front (arrows) represents the boundary between osteoid matrix (OM) and the mineralized bone matrix (MM). (Bar = 1 mm). (**b**) A view of the interfacial zone at higher magnification. Again an extracellular matrix rich in collagen fibers and foci of mineralization (*). OM = osteoid matrix, MM = mineralized matrix. (Bar = 500 μm)

with its surface [47]. After attachment of round cells from suspension, the following event is cell spreading. Regarding the cells morphology, early in the experiment, most of them adopt a rather polygonal shape, which is an osteoblasts feature indicative of greater adhesion compared to a round morphology [47, 48]. The rare elongated fibroblastic shapes are probably due to the treatment used to isolate cells: the dissolution of the extracellular matrix with the collagenase could have affected the early shape of seeded cells [42]. None of the cells examined shows a round shape, evidence of premature senescence or cellular suffering. The relevance of our results is underlined by other data obtained on primary osteoblasts in contact with biocompatible materials [49]. The early step of adhesion is really of great importance in the studies of biocompatibility. First interactions created between cells and materials surface control most aspects of subsequent cell behaviour such as morphology, migration, growth [50] and differentiation [47, 51, 52]. It is well established now that round cell morphology indicates cellular suffering, inducing decreased synthesis activity such as DNA or alkaline phosphatase production [48]. Moreover, if primary cells are grown in "non-appropriate" conditions, i.e. presence of stressing agents at cytotoxic level, they undergo premature senescence that is easily recognized by dramatic change in cell morphology [53]. Our SEM observations on primary cells do not show evidence of any gross alteration in cellular morphology. In addition, the close contact observed all along the experiment between metallic surface and osteoblastic cells is a sign of very good biocompatibility as discussed by Locci et al in the case of human osteoblasts cultured on plastic and titanium [54].

Concerning the buds seen on the dorsal surface of cells (Fig. 6c), we do not believe that they are associated with apoptosis since osteoblasts have polygonal or elongated shapes. Similar structures have been observed on HA-

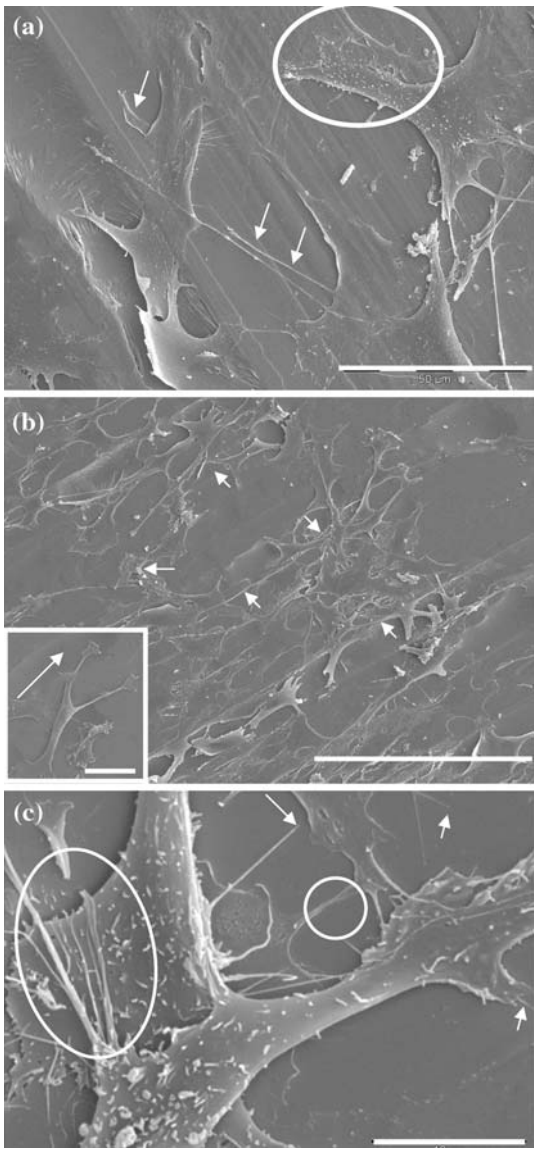

Fig. 6 SEM observations of osteoblastic cells, cultured on $Ti_{45}Zr_{38}Ni_{17}$ surface. (**a**) at 4 h, osteoblats adhere to the substrate with thin filopodia (white arrows), developing very intimate contact with the material. Ruffles on the dorsal surface of an osteoblastic cell reveal a synthesis activity (white circle) (Bar = 50 μm) (**b**) at 24 h, the cellular layer covers a large part of the surface: osteoblasts have proliferated and developed a network of communication. (Bar = 200 μm), in insert, an osteoblast displaying a polarized structure: the cell motivity is indicated by the white arrow with arrowhead corresponding to the cell front. (Bar = 50 μm), (**c**) at 48 h, observation of dense interconnections between osteoblasts (white circles). Contacts exist between cells and substrate as well (white arrows). The osteoblasts have an intense synthesis activity as visible on there cytoplasm: dorsal ruffles are evidence of extracellular matrix synthesis [31, 32] (Bar = 10 μm)

coated bioglass [31] and on metallic samples [32] and are assigned to matrix vesicles since osteoblastic cells were able to synthesize their extracellular matrix. These first results, both mostly polygonal shapes and bundling morphologies, highlight the positive interactions developed between primary osteoblasts and $Ti_{45}Zr_{38}Ni_{17}$ surface and suggest that our substrate is biocompatible.

Other evidence of this lack of cytotoxicity is the development of cells after adhesion and spreading. They can move and proliferate. The presence of polarized morphologies on our substrate is really positive, suggesting osteoblasts locomotion on $Ti_{45}Zr_{38}Ni_{17}$ surface. This phenomenon is crucial, not only because it confirms the short-term biocompatibility of the metallic surface, but also because cell locomotion plays an essential role in colonization of surfaces, for tissue engineering. When migrating, cells must first acquire a spatial asymmetry enabling them to turn intracellularly generated forces into net cell body translocation. An important consequence of polarization is that extension of active membrane processes, including both lamellipodia and filopodia, take place primarily around the cell front [55]. However, it should be kept in mind that locomotion is possible only if the cell attachment on the surface is just enough both to create positive interactions for next cellular development and to enable progressive cell motivity. From our observation, we can conclude that the interactions between osteoblasts and metallic surface respect this balance.

Concerning proliferation, it is thought that the early stage of cellular development is their ability to establish a cell-to-cell contact. Indeed, gap junctions connecting neighbouring cells ensure diffusion of inorganic ions and small molecules from one to another [47, 56]. The rich communication network developed by primary cells shows that $Ti_{45}Zr_{38}Ni_{17}$ provides an environment favourable for cell–cell interactions as well as cell-substrate interactions. Proliferation is thus possible in this context. Next steps of condensation and differentiation would be possible since cells adhere, are able to synthesize proteins, communicate and proliferate.

However, although SEM observations indicate the short-term biocompatibility of $Ti_{45}Zr_{38}Ni_{17}$ with respect to primary osteoblasts, the specific roles of various topographical (roughness), physical or chemical (corrosion) parameters of the surface, which plays a critical role in the cell/material interactions [57], could not be ruled out at this stage. Further research has to be done about the effects of $Ti_{45}Zr_{38}Ni_{17}$ surface on long-term cells development. The evaluation of the alkaline phosphatase activity, as well as cellular proliferation will be performed and compared to those obtained on different microstructures (crystallised, quasicrystallised) with the same composition so that effects of non periodical microstructures on osteoblasts would be evaluated. Nevertheless, from SEM observations, $Ti_{45}Zr_{38}Ni_{17}$ surface would not interfere with normal primary cells development, from adhesion to proliferation and development of cell-to-cell

contacts. This conclusion is promising since the first stages of a material integration are of great importance, determining its long-term biocompatibility.

5 Conclusion

In biomaterial research, mainly focused on cells responses to various substrate parameters, few studies concern the role of microstructure in cells behaviour. In the peculiar case of non periodical organisation, the choice of composition and the material characterization in term of structure appear as compulsory steps before investigating their hypothetic effects on biological materials. The ternary $Ti_{45}Zr_{38}Ni_{17}$ alloy, known to form complex microstructures by rapid solidification methods, has been hereby investigated. The as-quenched ribbons display a microstructure never reported before, mainly composed by an amorphous matrix with a low dispersion of nanometric β-phase particles. This composite nature would turn out to be promising in term of mechanical properties. Moreover, in-vitro experiments demonstrate that this non periodical structure has negligible effects on apparent osteoblastic cells behaviour since their development aren't affected by the presence of $Ti_{45}Zr_{38}Ni_{17}$, both at short and long terms. Osteoblasts adhere, spread, expressing numerous cytoplasmic digitations, and have a proliferation stage till condensation and differentiation. All our experiments consequently suggest that $Ti_{45}Zr_{38}Ni_{17}$ could be considered as a biocompatible system with respect to its chemical composition. In addition, mineralized nodules formation gives evidence of its specific bone compatibility.

Biocompatibility tests such as those performed in this study have only shown particular aspects of cell behaviour, based on morphological observations (adhesion, differentiation, and mineralization). The cell reaction to an implant is however a very complex situation. In order to have a more quantitative description of the cell/material interactions in term of cell attachment strength, proliferation rate, differentiation, assays of proteins (vinculin, phosphatise alkaline, osteocalcin) represent the next step of this study, notably to accurately characterize the effects of such peculiar microstructure on osteoblasts development.

Acknowledgements This work was supported by grants from the Centre National de la Recherche Scientifique, the Slovak Grant Agencies (VEGA 5/5096/25, APVT-51-052702) and SAS Centre of Excellence "Nanosmart. H. L. is grateful to the SMATEC company (Belgium) and the CNRS for providing her doctorate scholarship. The authors would like to thank the Slovak Academy of Sciences (SAV, Bratislava), specially the Department of Metal Physics for experimental support and fruitful discussions, as well as G. Wang (CECM, Vitry/France) and J. Y. Laval (ESPCI, Paris/France) for giving them access to transmission electron microscopes, D. Montero (Service de microscopie électronque à balayage Paris 7-Laboratoire de Biologie du Développement, Paris/France) and M. Oboeuf for their technical assistance in SEM and TEM preparation.

References

1. P. I. BRANEMARK, B. O. HANSSON, R. ADELL, U. BREINE, J. LINDSTRÖM, O. HALLEN and A. OHMAN, *Scan. J. Plast. Reconstr. Surg.* **16** (1977) 1
2. V. BIEHL and J. BREME, *Mat.-wiss. u. Werkstofftech.* **32** (2001) 137
3. C. SCHMIDT, D. KASPAR, M. R. SARKAR, L. E. CLAES, A. A. IGNATIUS, *J. Biomed. Mater. Res. (Appl. Biomater.)* **63** (2002) 252
4. D. F. WILLIAMS, *J. Med. Eng. Tech.* **6** (1977) 202
5. D. F. WILLIAMS, *J. Med. Eng. Tech.* **6** (1977) 266
6. E. LAUTENSCHLAGER and P. MONAGHAN, *Int. Dent. J.* **43** (1993) 245
7. A. SCHEDLE, P. SAMORAPOOMPICHIT, X. H. RAUSCHFAN, A. FRANZ, W. FUREDER, W. R. SPERR, W. SPERR, A. ELLINGER, R. SLAVICEK, G. BOLTZ-NITULESCU and V. VALENT, *J. Dent. Res.* **74** (1995) 1513
8. E. J. EVANS, *Biomaterials* **15** (1994) 713
9. M. BRAMA, N. RHODES, J. HUNT, A. RICCI, R. TEGHIL, S. MIGLIACCIO, C. DELLA ROCCA, S. LECCISOTTI, A. LIOI, M. SCANDURRA, G. DE MARIA, D. FERRA, F. PU, G. PANZINI, L. POLITI and R. SCANDURRA, *Biomaterials* **27** (2007) 595
10. X. LIU, P. K. CHU and C. DING, *Mater. Sci. Eng.* **R47** (2004) 49
11. S. PISCANEC, L. COLOMBI CIACCHI, E. VESSELLI, G. COMELLI, O. SBAIZERO, S. MERIANI and A. DE VITA, *Acta Mater.* **52** (2004) 1237
12. T. SAWASE, K. YOSHIDA, Y. TAIRA, K. KAMADA, M. ATSUTA and K. BABA, *J. Oral Rehab.* **32** (2005) 151
13. A. C. FERNANDES, F. VAZ, E. ARIZA, L. A. ROCHA, A. R. L. RIBEIRO, A. C. VIEIRA, J. P. RIVIERE and L. PICHON, *Surf. Coat. Tech.* **2000** (2006) 6218
14. M. CALVO-DAHLBORG, *Mater. Sci. Eng.* **A226–228** (1997) 833
15. A. INOUE, *Mater. Sci. Eng. A.* **304–306** (2001) 1
16. A. INOUE, *Intermetallics* **8** (2000) 455
17. A. INOUE, C. FAN, J. SAIDA and T. ZHANG, *Sci. Tech. Adv. Mater.* **1** (2000) 73
18. S. FAGHIHI, F. AZARI, H. LI, M. R. BATENI, J. A. SZPUNAR, H. VALI and M. TABRIZIAN, *Biomaterials* **27** (2006) 3532
19. J. LINCKS, B. D. BOYAN, C. R. BLANCHARD, C. H. LOHMANN, Y. LIU, D. L. COCHRAN, D. D. DEAN and Z. SCHWARTZ, *Biomaterials* **19** (1998) 2219
20. A. PECKER and W. L. JOHNSON, *Appl. Phys. Lett.* **63** (1993) 2342
21. L. WANG, L. MA, C. MA and A. INOUE, *J. Alloys Compd.* **361** (2003) 234
22. N. CHEN, D. V. LOUZGUINE, S. RANGANATHAN and A. INOUE, *Acta Mater.* **53** (2005) 759
23. J. P. DAVIS, E. H. MAJZOUB, J. M. SIMMONS and K. F. KELTON, *Mater. Sci. Eng.* **A294–296** (2000) 104
24. J. B. QIANG, Y. M. WANG, D. H. WANG, M. KRAMER, P. THIEL and C. DONG, *J. Non-Cryst. Sol.* **334&335** (2004) 223
25. K. F. KELTON, W. J. KIM and R. M. STROUD, *Appl. Phys. Lett.* **70** (1997) 3230
26. J. BASU, D. V. LOUZGUINE, A. INOUE and S. RANGANATHAN, *J. Non-Cryst. Sol.* **334&335** (2004) 270
27. H. LEFAIX, F. PRIMA, P. DUBOT, D. JANICKOVIK and P. SVEC, *Mater. Sci. Eng.* **A449–451** (2007) 995
28. H. LEFAIX, F. PRIMA, S. ZANNA, P. VERMAUT, P. DUBOT, P. MARCUS, D. JANICKOVIK and P. SVEC, *Mater. Trans. JIM* **48** (2007) 1

29. H. DECLERCQ, N. VAN DEN VREKEN, E. DE MAEYER, R. VERBEECK, E. SCHACHT, L. DE RIDDER and M. CORNELISSEN, *Biomaterials* **25** (2004) 757
30. H. DECLERCQ, R. VERBEECK, L. DE RIDDER, E. SCHACHT and M. CORNELISSEN, *Biomaterials* **26** (2005) 4964
31. I. D. XYNOS, M. V. J. HUKKANEN, J. J. BATTEN, L. D. BUTTERY, L. L. HENCH and J. M. POLAK, *Calcif. Tissue Int.* **67** (2000) 321
32. J. VAN DES DOLDER, W. JWM, P. H. M. SPAUWEN and J. A. JANSEN, *J. Biomed. Mater. Res.* **62** (2002) 350
33. A. INOUE, H. M. KIMURA and T. ZHANG, *Mater. Sci. Eng.* **294–296** (2000) 727
34. F. SCHURACK, J. ECKERT and L. SCHULTZ, *Mat. Sci. Eng.* **294–296** (2000) 164
35. D. J. SORDELET, E. ROZHAKOVA, M. F. BESSER and M. J. KRAMER, *J. Non-Cryst. Sol.* **334&335** (2004) 263
36. K. F. KELTON, A. K. Gangopadhyay, G. W. LEE, L. HANNET, R. W. HYERS, S. KRISHNAN, M. B. ROBINSON, J. ROGERS and T. J. RATHZ, *J. Non-Cryst. Sol.* **312–314** (2002) 305
37. K. F. KELTON, *J. Non-Cryst. Sol.* **334–335** (2004) 253
38. A. TAKASAKI and K. F. KELTON, *J. Alloys Compnd.* **347** (2002) 295
39. A. TAKASAKI and K. F. KELTON, *J. Hydrogen Energy* **31** (2006) 183
40. E. HUTTUNEN-SAARIVIRTA, *J. Alloys Compd.* **363** (2004) 150
41. C. J. KIRKPATRICK and C. MITTERMAYER, *J. Mater. Sci. Mater. Med.* **1** (1990) 9
42. J. M. SAUTIER, J. R. NEFUSSI and N. FOREST, *Bio. Cell.* **78** (1993) 181
43. S. LOTY, C. FOLL, N. FOREST and J. M. SAUTIER, *Arch. Oral Biol.* **45** (2000) 843
44. T. M. LEE, E. CHANG and C. Y. YANG, *Biomaterials* **25** (2004) 23
45. S. HATTAR, A. ASSELIN, D. GREENSPAN, M. OBOEUF, A. BERDAL and J. M. SAUTIER, *Biomaterials* **26** (2005) 839
46. D. E. STEFLIK, R. S. CORPE, F. T. LAKE, T. R. YOUNG, A. L. SISK, G. R. PARR, P. J. HANES and D. J. BERKERY, *J. Biomed. Mater. Res.* **39** (1998) 611
47. K. ANSELME, *Biomaterials* **21** (2000) 667
48. J. FOLKMAN, A. MOSCONA, *Nature* **273** (1978) 345
49. R. CARBONE, I. MARANGI, A. ZANARDI, L. GIORGETTI, E. CHIERICI, G. BERLANDA, A. PODESTA, F. FIORENTINI, G. BONGIORNO, P. PISERI, P. G. PELICCI and P. MILANI, *Biomaterials* **27** (2006) 3221
50. M. BIGERELLE and K. ANSELME, J. Biomed. Mate. Res. **72A** (2005) 36
51. A. BOUAFSOUN, A. OTHMANE, A. KERKENI, N. JAFFREZIC and L. PONSONNET, *Mater. Sci. Eng.* **C66** (2006) 260
52. B. M. GUMBINER, *Cell* **84** (1996) 345
53. J. MA, H. WONG, L. B. KONG and K. W. PENG, *Nanotechnology* **14** (2003) 619
54. P. LOCCI, L. MARINUCCI, C. LILLI, S. BELCASTRO, N. STAFFOLANI, S. BELLOCCHIO, F. DAMIANI and E. BECCHETTI, *J. Biomed. Mater. Res.* **51** (2000) 561
55. D. A. LAUFFENBURGER and A. F. HORWITZ, *Cell* **84** (1996) 359
56. N. M. KUMAR and N. B. GIGULA, *Cell* **84** (1996) 381
57. B. KASEMO, *Surf. Sci.* **500** (2002) 61